DEVELOPMENT OF AN ADVANCED MONITORING APPLICATION FOR GEOTHERMAL POWER PLANTS WITH AN ORGANIC RANKINE CYCLE

Matthäus Irl[1]*, Christoph Wieland[12], Hartmut Spliethoff[13]

[1]Technical University of Munich, Chair of Energy Systems, Garching, Bavaria, Germany

[2]Technical University of Munich, Munich School of Engineering, Garching, Bavaria, Germany

[3]Bavarian Center for Applied Energy Research, Garching, Bavaria, Germany

*Corresponding Author: matthaeus.irl@tum.de

ABSTRACT

Renewable power generation technologies are becoming increasingly important. One of these technologies is electricity production with an Organic Rankine Cycle supplied by the heat of deep hydro-geothermal plants. They produce electrical power with a high annual full load hour percentage and comparatively low CO_2 emissions. However, since the geothermal plants are operated with air-cooled condensers as well as scaling affects the performance of the electrical submersible pump and thus the lifted thermal water flow rate, the generated gross electrical power is strongly fluctuating. Therefore, the process parameters of the main components heat exchanger, turbine and condenser of an Organic Rankine Cycle as part of a geothermal plant are highly variable, both in terms of diurnal and seasonal fluctuations. Monitoring an Organic Rankine Cycle is therefore associated with special challenges for geothermal power plant operators.

For advanced monitoring of the operation of the main components heat exchanger, turbine and condenser of geothermal power plants, a methodology with developed analytical and empirical simulation models is presented in this paper. For a shell-and-tube evaporator of a reference geothermal power plant in the South Bavarian Molasse Basin with a two-stage Organic Rankine Cycle, an equation-based simulation model for the calculation of the thermal resistance due to scaling and fouling in the thermal brine circuit is shown. The analysis of more than three years of operation of the shell-and-tube evaporator in the high-temperature circuit of an ORC reference geothermal plant shows a minimal thermal resistance due to scaling and fouling for the whole period, which indicates that scaling and fouling did not have a strong influence on heat transfer.

Furthermore, empirical simulation models based on linear regression developed for the turbines of the reference geothermal power plant with a two-stage Organic Rankine Cycle are presented. The isentropic turbine efficiency is determined with a two-dimensional polynomial function of the simulation model, whose regression coefficients are calculated numerically. For this purpose, operational data from a three-year period of the reference geothermal power plant with a two-stage Organic Rankine Cycle in the south of Munich (Germany) were preprocessed and used. Polynomial functions of various degrees and different objective functions for the numerical computation of regression coefficients are examined. Regression models for three years of operation of the investigated geothermal plant were computed and compared with each other. The same methodology as for monitoring the operation of the turbines is applied to monitor the performance of the air condenser of a geothermal power plant. In addition, results of applying this methodology by retro perspective analysis of the operational data of the reference geothermal power plant are processed, which show no negative changes in the operation of the turbines and air-cooled condensers in both circuits of the ORC reference geothermal power plant.

A software application is presented, developed with the MATLAB® App Designer that integrates the developed methodology and the simulation models of the main components. For realtime operation monitoring, the current process parameters of the main components of the Organic Rankine Cycle of

the reference geothermal power plant can be specified, which are evaluated comparatively with the calculated key performance indicator values of the empirical models of each operation year or of the analytical models. Thus, the developed software tool facilitates operators to easily and precisely monitor the operation of the main components of an Organic Rankine Cycle of their geothermal power plant.

1 INTRODUCTION

With the European Climate Law, the European Commission proposes a legally binding target of net zero greenhouse gas emissions by 2050 (European Commission, 2021) due to the fast climate change mitigation (World Meteorological Organization, 2021). Therefore, power generation from renewable energy resources becomes increasingly important, as CO2 emissions of renewable power generation technologies are very low. The exploitation of deep hydro-geothermal energy is a comparatively young technology for the supply with electricity and heat with low CO_2 emissions. Over the past 15 years, Munich, and in particular the southern Munich region has developed into a hotspot for the expansion and utilization of deep hydro-geothermal energy in Germany. Mraz (2019) pointed out that the karstic limestone aquifer of the South Bavarian Molasse Basin offers suitable geological conditions for the utilization of deep hydro-geothermal energy in southern Bavaria. According to the German Geothermal Association (2021), today two geothermal power plants and four geothermal plants with combined heat and power production are there in operation. Five of these geothermal power plants are equipped with an Organic Rankine Cycle as a binary thermodynamic cycle. Four of the five geothermal power plants have been built with a two-stage Organic Rankine Cycle, which is more complex with more components compared to the single-stage Organic Rankine Cycle.

The main process parameters and thus the gross electrical power output of these geothermal power plants in the South Bavarian Molasse Basin as well as of air-cooled Organic Rankine Cycle geothermal power plants in general are highly fluctuating for the following reasons (Irl *et al.*, 2021):

- The outlet pressure of the backpressure turbine fluctuates strongly due to the wide range of the condensing temperature and pressure of the air-cooled condensers. The turbine outlet pressure sets the usable enthalpy difference across the turbine because the inlet process parameters of the turbine are nearly constant. Since the ambient air temperature varies considerably both throughout the day and seasonally, the generated gross electrical power fluctuates equally.
- The thermal energy of the thermal brine is primarily used to supply the geothermal heating plant, since in this paper considered geothermal power plants with combined heat and power production are operated on a heat-driven basis. The fluctuations in the thermal power of the district heating system of the geothermal plant cause in turn fluctuations in the thermal brine mass flow rate that can be supplied to the power cycle of a geothermal power plant.
- In previous work, it was shown that the flow rates of the thermal brine of electrical submersible pumps with high flow rates used in geothermal plants with power production reduce with increasing operating time (Irl *et al.*, 2020). The reason for this is scales, which are mineral deposits, in the electrical submersible pumps. The scales deteriorate the hydraulic efficiency of the electrical submersible pumps and thus the flow rate (Köhl *et al.*, 2020). A lower thermal brine flow rate causes a lower thermal power available to the geothermal power plant for power generation.

The highly fluctuating process parameters of the Organic Rankine Cycles make it difficult for geothermal plant operators to evaluate and assess the operating states of the main components of their Organic Rankine Cycle power plants. In a literature review, no previous work concerning the monitoring of air-cooled Organic Rankine Cycle power plants could be found that could have been built upon. The own research of the authors has shown that the existing process control systems of Organic Rankine Cycle power plants have only limited functionality regarding monitoring. Manufacturers of Organic Rankine Cycle power plants often define limit values of measured values of the main components, which may not be exceeded or fallen below, and which were essentially defined only for safety-related aspects but are not suitable for sufficient monitoring of the main components. An advanced monitoring application for the power and efficiency as the main key performance indicators of air-cooled geothermal power plants with an Organic Rankine Cycle is presented as previous research in Irl *et al.* (2021).

2 METHODOLOGY

In this section, the applied methodology for the development of an advanced monitoring application for geothermal power plants with an Organic Rankine Cycle is described. Firstly, the measurement and operational data of a reference geothermal plant with combined heat and power production are pre-processed and validated. The reference geothermal power plant is located in the south of Munich and equipped with a two-stage Organic Rankine Cycle. More details on the reference geothermal power plant with combined heat and power production as well as on the two-stage Organic Rankine Cycle can be found in Irl *et al.* (2021). Subsequently, an equation-based steady-state simulation model with numerical computation of the HT-evaporator is developed to calculate the thermal resistance due to scaling and fouling as the main key performance indicator of this component. For the turbines and the air-cooled condensers empirical simulation models are developed by means of linear regression with the operational data for each year of operation of the reference geothermal plant to calculate the isentropic efficiencies and the condensing temperatures dependent on their main influencing process parameters with different polynomial and objective functions for the numerical computation of the polynomial coefficients. In the next step, suitable polynomial functions are selected for the simulation models, followed by a retro perspective analysis of the operation of the main components of the reference geothermal power plant. Finally, the monitoring software application is programmed, including the design of a user interface and the integration of the developed simulation models, which facilitates operators to easily and precisely monitor the operation of the main components of an Organic Rankine Cycle of their geothermal power plant.

3 SHELL-AND-TUBE EVAPORATOR OPERATION MONITORING

3.1 Development of an Equation-based Simulation Model with Numerical Computation

Figure 1 shows the schematic structure of the equation-based steady-state simulation model of the shell-and-tube evaporator in the high-pressure circuit of the ORC reference geothermal power plant. The shell-and-tube evaporator is divided into its four tube passes for the simulation model. The thermal brine flows horizontally in the tubes and is turned round 180° three times. The working fluid enters in a liquid state through two nozzles at the bottom of the evaporator and exits as saturated vapor at the top.

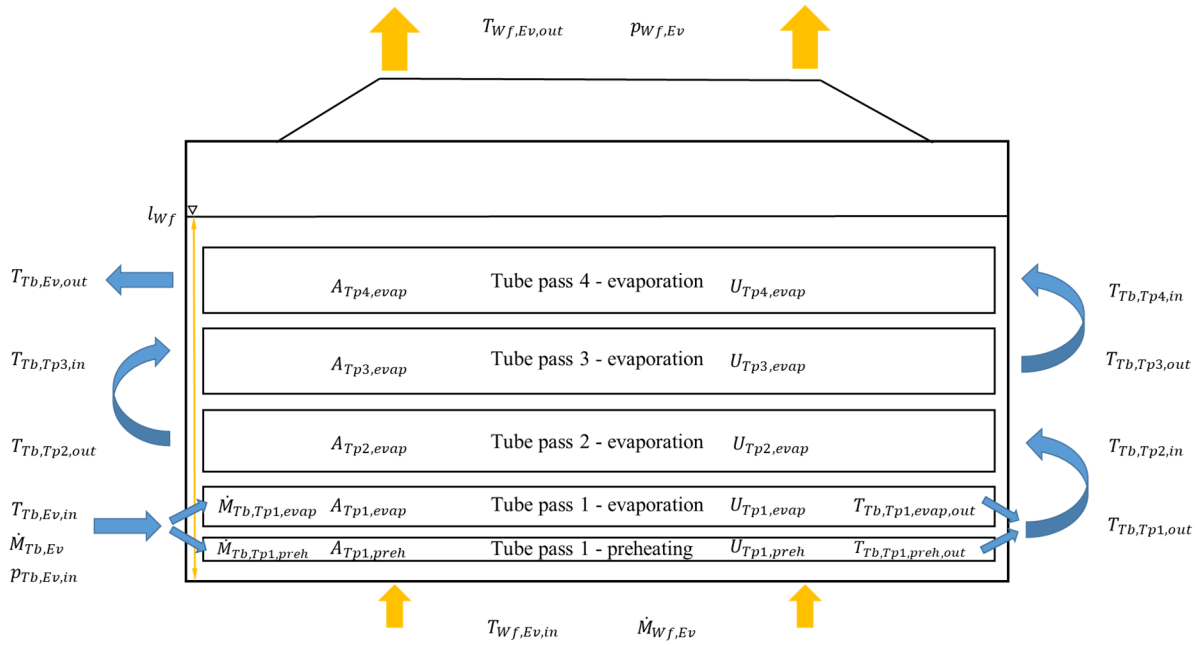

Figure 1: Schematic structure of the equation-based steady-state simulation model of the shell-and-tube evaporator in the high-pressure circuit of the ORC reference geothermal power plant

A heat exchanger equation is set up for each tube pass using the Effectiveness-NTU Method, which is described in Karwa (2020). The first tube pass is again divided into two segments: The first segment preheats the working fluid up to the saturation temperature $T_{Wf,Ev,sat}$. For this purpose, a cross-flow with mixed thermal brine and unmixed working fluid according to Smith (1934) was modeled in Equation (1). In Equations (2) and (3), the mass and area balances are set up for the first tube pass. The thermal brine mass flow is divided pro rata to both segments of the first tube pass according to Equation (4). The thermal power $\dot{Q}_{Tb,Tp1,preh}$ required for preheating is given to the simulation model as an input variable, which according to Equation (5) corresponds to the energy balance of the segment for preheating of the first tube pass. According to Karwa (2020), Equation (6) is applied to model the heat transfer of the second segment of the first tube pass, in which the fully preheated working fluid evaporates and the heat capacity flow of the working fluid approaches infinity. Equation (8) describes the heat transfer of evaporation for the following three tube passes. The heat transfer coefficient for the pool nucleate boiling on the outside wall of the tube for the second segment of the first tube pass according to Cooper (1984) is given in Equation (7), which is dependent on the heat flux density and thus on the transferred heat power. Similarly, according to Equation (9), the pool nucleate boiling heat transfer coefficient is modeled for the three other tube passes. Thus, the system of equations to be solved for the steady-state simulation model consists of 13 equations in total.

$$\frac{T_{Tb,Ev,in}-T_{Tb,Ev,Tp1,preh,out}}{T_{Tb,Ev,in}-T_{Wf,Ev,in}} = 1 - exp\left(\frac{exp\left(-\frac{\dot{M}_{Tb,Tp1,preh}\cdot c_{Tb,Tp1,preh,m}}{\dot{M}_{Wf,Ev,in}\cdot c_{Wf,Tp1,preh,m}}\frac{U_{Tp1,preh}\cdot A_{Tp1,preh}}{\dot{M}_{Tb,Tp1,preh}\cdot c_{Tb,Tp1,preh,m}}\right)-1}{\frac{\dot{M}_{Tb,Tp1,preh}\cdot c_{Tb,Tp1,preh,m}}{\dot{M}_{Wf,Ev,in}\cdot c_{Wf,Tp1,preh,m}}}\right) \quad (1)$$

$$A_{Tp1} = A_{Tp1,preh} + A_{Tp1,evap} \quad (2)$$

$$\dot{M}_{Tb,Tp1} = \dot{M}_{Tb,Tp1,preh} + \dot{M}_{Tb,Tp1,evap} \quad (3)$$

$$\dot{M}_{Tb,Tp1,preh} = \dot{M}_{Tb,Tp1}\cdot\frac{A_{Tp1,preh}}{A_{Tp1}} \quad (4)$$

$$\dot{Q}_{Tb,Tp1,preh} = \dot{M}_{Tb,Tp1,preh}\cdot\left(H_{Tb,Ev,in}\left(T_{Tb,Ev,in},p_{Tb,Ev,in}\right) - H_{Tb,Tp1,preh,out}\left(T_{Tb,Tp1,preh,out},p_{Tb,Tp1,preh,out}\right)\right) \quad (5)$$

$$\frac{T_{Tb,Ev,in}-T_{Tb,Tp1,evap,out}}{T_{Tb,Ev,in}-T_{Wf,Ev,sat}} = 1 - exp\left(\frac{U_{Tp1,evap}\cdot A_{Tp1,evap}}{\dot{M}_{Tb,Tp1,evap}\cdot c_{Tb,Tp1,evap,m}}\right) \quad (6)$$

$$\alpha_{Wf,Tp1,evap} = 55\cdot\left(\frac{p_{Wf,Ev}}{p_{Wf,c}}\right)^{0.12-0.087\cdot\ln(\varepsilon)}\cdot\left(-0.4343\cdot\ln\left(\frac{p_{Wf,Ev}}{p_{Wf,c}}\right)\right)^{-0.55}\cdot\frac{1}{\sqrt{M_{Wf}}}\cdot\left(\frac{\dot{M}_{Tb,Tp1,evap}\cdot\left(H_{Tb,Ev,in}(T_{Tb,Ev,in},p_{Tb,Ev,in})-H_{Tb,Tp1,evap,out}(T_{Tb,Tp1,evap,out},p_{Tb,Tp1,evap,out})\right)}{A_{Tp1,evap}}\right)^{0.67} \quad (7)$$

$$\frac{T_{Tb,Tpx,in}-T_{Tb,Tpi,out}}{T_{Tb,Tpx,in}-T_{Wf,Ev,sat}} = 1 - exp\left(\frac{U_{Tpx,evap}\cdot A_{Tpx,evap}}{\dot{M}_{Tb,Tpx,evap}\cdot c_{Tb,Tpx,evap,m}}\right) \quad (8)$$

$$\alpha_{Wf,Tpx,evap} = 55\cdot\left(\frac{p_{Wf,Ev}}{p_{Wf,c}}\right)^{0.12-0.087\cdot\ln(\varepsilon)}\cdot\left(-0.4343\cdot\ln\left(\frac{p_{Wf,Ev}}{p_{Wf,c}}\right)\right)^{-0.55}\cdot\frac{1}{\sqrt{M_{Wf}}}\cdot\left(\frac{\dot{M}_{Tb,Tpx,evap}\cdot\left(H_{Tb,Tpx,in}(T_{Tb,Tpx,in},p_{Tb,Tpx,in})-H_{Tb,Tpx,evap,out}(T_{Tb,Tpx,out},p_{Tb,Tpx,out})\right)}{A_{Tpx,evap}}\right)^{0.67} \quad (9)$$

$$U_{Tpx,evap} = \left(\frac{1}{\alpha_{Tb,Tpx}}\cdot\frac{d_{Tu,od}}{d_{Tu,id}} + R_{Tb,SaF,m}\cdot\frac{d_{Tu,od}}{d_{Tu,id}} + \frac{d_{Tu,od}\cdot\ln\left(\frac{d_{Tu,od}}{d_{Tu,id}}\right)}{2\cdot\lambda_{Tu}} + \frac{1}{\alpha_{Wf,Tpx,evap}}\right)^{-1} \quad (10)$$

Equation (10) represents the heat transfer coefficient of each tube pass with evaporation. The heat transfer coefficient of the turbulent tube flow of thermal brine $\alpha_{Tb,Tpx}$ is calculated according to Gnielinski (1975). Finally, the average thermal resistance due to scaling and fouling $R_{Tb,SaF,m}$ for the evaporator in Equation (10) can be computed applying the system of equations. Due to the small number of equations, the simulation model can be easily set up by geothermal power plant operators and can be

numerically calculated with common solvers without expensive special software and high computing capacity. For the calculation, the function *fmincon* of the software MATLAB® by Mathworks is used.

3.2 Results of the Analysis of Three Years of Operation

The simulation model described in Section 3.1 is used to calculate the average thermal resistance due to scaling and fouling of the shell-and-tube evaporator of the high-pressure circuit of the ORC reference geothermal power plant for an operating period of several years. Input variables of the simulation model from the operating data of the ORC reference geothermal power plant are the mass flows of both fluids, the inlet and outlet temperatures with associated pressures of the thermal brine, the inlet temperature of the working fluid, and the calculated thermal power for complete preheating of the working fluid. All input variables are passed to the simulation model as weekly average values.

Figure 2 shows the calculated average thermal resistance due to scaling and fouling, as well as the calculated area-averaged overall heat transfer coefficient for the operating period from May 2015 to the end of 2018. As can be seen, the calculated values of the average thermal resistance due to scaling and fouling are in the slightly negative range close to zero for most of the period. Physically, negative values

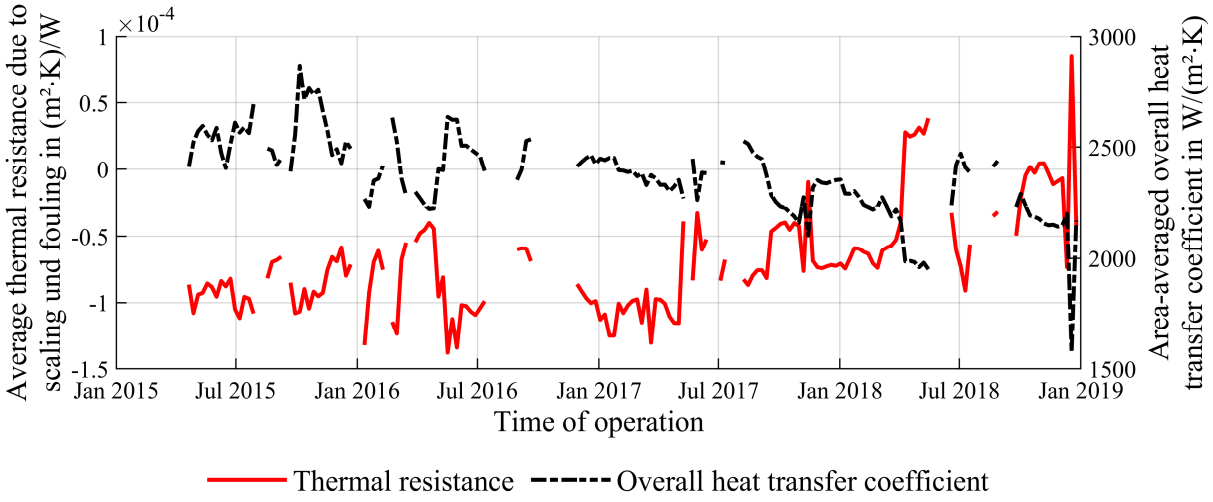

Figure 2: Time curves of the computed average thermal resistance due to scaling and fouling and the computed area-averaged overall heat transfer coefficient of the shell-and-tube evaporator in the high-pressure circuit of the ORC reference geothermal power plant

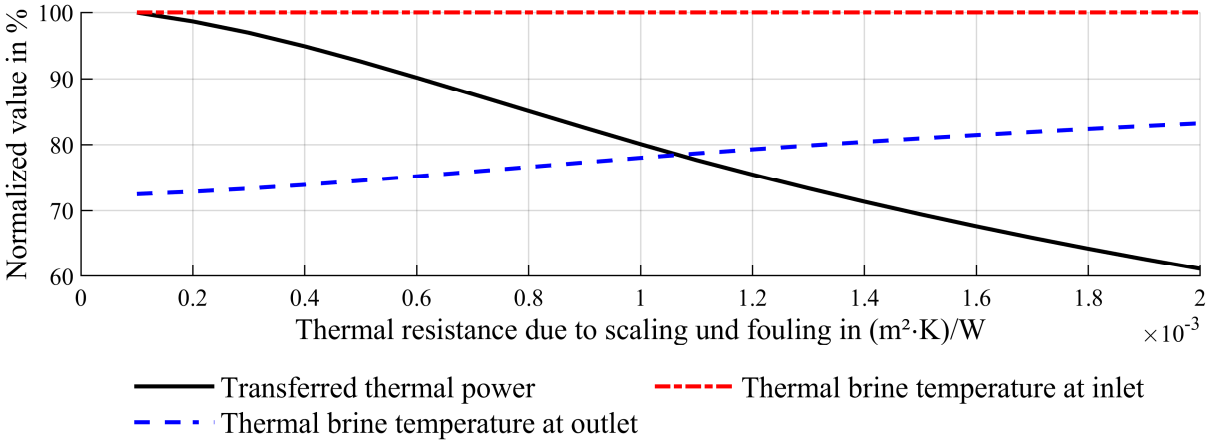

Figure 3: Thermal power and thermal brine outlet temperature as a function of the thermal resistance due to scaling and fouling of the shell-and-tube evaporator in the high-pressure circuit of the ORC reference geothermal power plant

of thermal resistance due to scaling and fouling are not possible. The reason for this result is not an accurate representation of the reality of the simulation model. However, since the values are close to

zero, the deviation is considered minor. The decisive result is the minimal increase in average thermal resistance due to scaling and fouling during the operating period, which indicates that scaling and fouling did not have a strong influence on heat transfer. This is also shown by the moderate change in the overall heat transfer coefficient values in Figure 2.

4 TURBINE OPERATION MONITORING

4.1 Development of an Empirical Simulation Model with Numerical Computation

A key performance indicator for monitoring the operation of turbines is the isentropic turbine efficiency in Equation (11). For the empirical simulation model, the difference in the inlet and outlet enthalpy of the working fluid at the turbine and the mass flow of the working fluid through the turbine are chosen as input variables. For the simulation model calculating the isentropic turbine efficiency, various polynomial functions are computed numerically with the operational data. The mass flow of the working fluid is considered in the polynomial functions in degree 1, the enthalpy difference in degrees 1 to 4. In total, this results in four different polynomial functions with 3 to 9 polynomial coefficients since mixed terms of the mass flow and the enthalpy difference of the working fluid are also taken into account in the polynomial functions.

$$\eta_{T,is} = \frac{h_{T,Wf,in} - h_{T,Wf,out}}{h_{T,Wf,in} - h_{T,Wf,out,is}} \tag{11}$$

The coefficients of all polynomial functions are computed numerically for two objective functions to be minimized according to Equations 12 and 13, for which the MATLAB® function *fmincon* is applied.

$$\min(\mathrm{LAR}_{\eta_{T,is,op,mo}}) = \sum_{i_{op}=1}^{j_{op}} \left|\eta_{T,is,op,i} - \eta_{T,is,op,mo,i}\right| \tag{12}$$

$$\min\left(\mathrm{RMSE}_{\eta_{T,is,op,mo}}\right) = \sqrt{\frac{1}{j_{Op}} \cdot \sum_{i_{op}=1}^{j_{Op}} \left(\eta_{T,is,op,i} - \eta_{T,is,op,mo,i}\right)^2} \tag{13}$$

According to Equation (12), the sum of the difference in magnitude of all residuals of the calculated isentropic turbine efficiency of the model is minimized (LAR), whereas according to Equation (13), the root mean square error of all residuals of the model is minimized (RMSE). Hence, in the model with the objective function according to Equation (13), larger deviations of the isentropic turbine efficiency calculated by the model are taken into account to a greater degree than in the model with the objective function according to Equation (12).

Table 1 shows the calculated RMSEs of all simulation models for the high-pressure turbine of the ORC reference geothermal power plant. With a polynomial function according to Equation (14), in which the enthalpy difference is included to the third power and which is optimized for the smallest sum of the difference in magnitude of all residuals, the best results can be achieved for both the high-pressure and the low-pressure turbine.

Table 1: Calculated RMSEs of all simulation models for the high-pressure turbine of the ORC reference geothermal power plant

Simulation model / Polynomial function	poly 11	poly 12	poly 13	poly 14
Year 2016, LAR	2.54	2.14	2.13	5.43
Year 2016, RMSE	2.53	2.13	2.20	2.64
Year 2017, LAR	2.75	2.21	2.20	26.36
Year 2017, RMSE	2.74	2.20	2.19	2.22
Year 2018, LAR	2.70	2.12	2.10	5.79
Year 2018, RMSE	2.67	2.11	2.16	2.14

$$\eta_{T,is,op,mo,i} = c_1 + c_2 \cdot \dot{m}_{Wf,i} + c_3 \cdot \Delta h_{T,i} + c_4 \cdot \dot{m}_{Wf,i} \cdot \Delta h_{T,i} + c_5 \cdot {\Delta h_{T,i}}^2 + c_6 \cdot \dot{m}_{Wf,i} \cdot {\Delta h_{T,i}}^2 + c_7 \cdot {\Delta h_{T,i}}^3 \tag{14}$$

4.2 Results of the Analysis of Three Years of Operation

Figure 4 shows the computed maps of the normalized isentropic turbine efficiency of the HT-circuit of the ORC reference geothermal power plant for the operating years 2016 and 2018. The computed maps show an approximate congruence. Figure 5 shows the differences of the computed maps of the operating years 2018 and 2016, and of the operating years 2018 and 2017. In the range of the maps with a high frequency of operating points, the differences correspond approximately to the calculated RMSEs in Table 1 that reveals a constant operation efficiency of the HT-turbine. The same results are obtained by evaluating the operation of the LT-turbine.

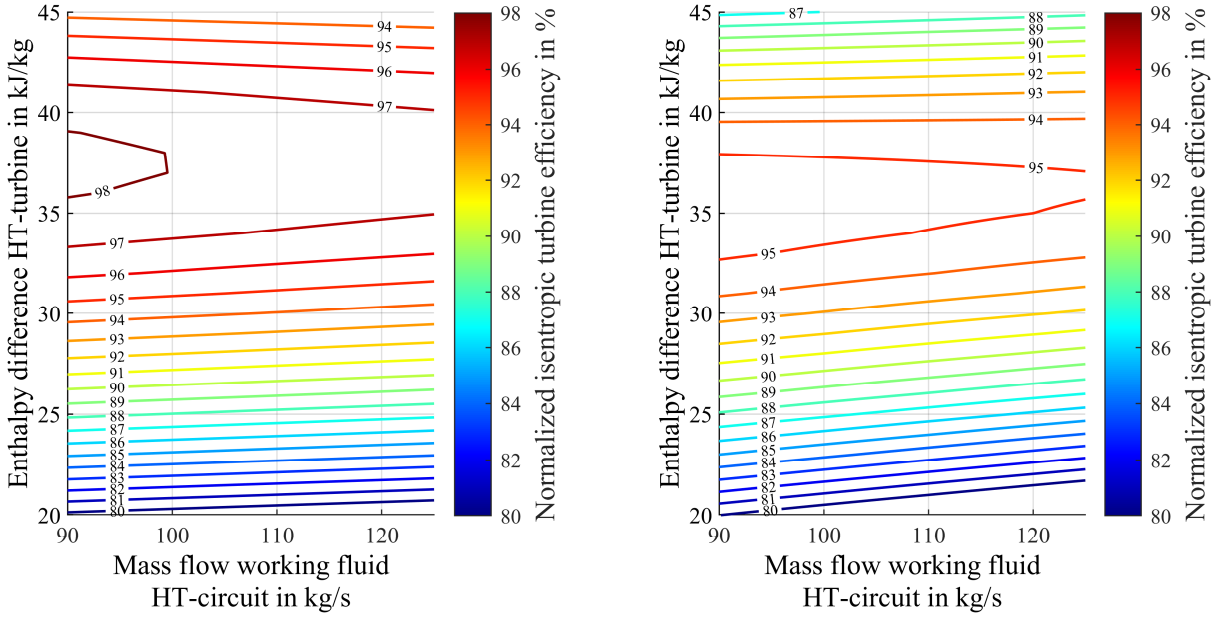

Figure 4: Computed maps for the operating years 2016 (left) and 2018 (right) of the HT-turbine of the ORC reference geothermal power plant

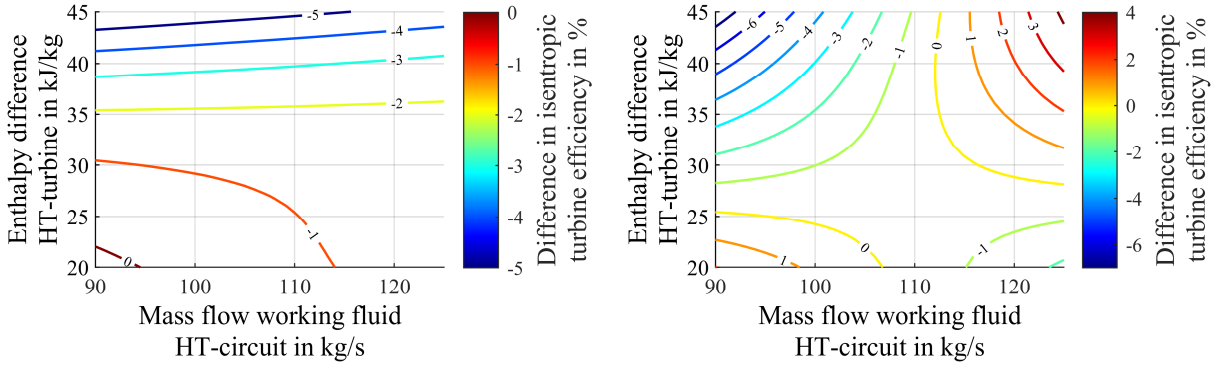

Figure 5: Difference of the computed maps of the operating years 2018 and 2017 (left), and 2018 and 2016 (right) of the HT-turbine of the ORC reference geothermal power plant

5 AIR-COOLED CONDENSER OPERATION MONITORING

The same methodology for the development of an empirical simulation model for monitoring the operation of the turbines in Section 4 is also applied to monitor the operation of the air-cooled condensers of the ORC reference geothermal power plant. Similarly, maps with polynomial functions of different degrees are computed numerically with the operational data for the two objective functions in Equations (12) and (13). Simulation models are developed calculating the condensing temperature as a function of the thermal power for desuperheating and condensation of the working fluid and the

ambient air temperature, which corresponds to the inlet temperature of the air condensers, again for both circuits. The best results for the calculation of the condensing temperature for the whole map is obtained with a linear dependence of both the thermal power for desuperheating and condensation of the working fluid and the ambient air temperature with the smallest RMSE as the objective function according to Equation (13) of the models of all operating years. The RMSEs of the HT-condenser of the simulation models of the individual operating years amount to 1.5 - 1.6 °C, and those of the LT-circuit to 1.5 - 1.8 °C. The comparison of the simulation models of the individual operating years shows deviations in the range of the calculated RMSEs of the models. Thus, it is proved that there were no changes in the operation during the analyzed three years of operation.

6 SOFTWARE APPLICATION FOR MONITORING THE KEY PERFORMANCE INDICATORS OF THE MAIN COMPONENTS OF THE ORC REFERENCE GEOTHERMAL POWER PLANT

In a final step, the developed simulation models from Section 3-5 are applied in a software application that allows the operator of the reference geothermal plant to permanently monitor the thermal resistance due to scaling and fouling of the HT-evaporator, the isentropic turbine efficiencies of both turbines and the condensing temperatures of both air-cooled condensers. The software application was developed using MATLAB® App Designer and compiled into a stand-alone executable file. In the user interface of the software application, the user can enter the inlet and outlet temperature of the thermal brine of the HT-evaporator, the inlet temperature of the working fluid of the HT-evaporator, the mass flows of the thermal brine in the HT-circuit and of the working fluids in the HT- and LT-circuit, the pressures inside the evaporators and after the turbines as well as in the condensers of both circuits, the turbine inlet and outlet temperatures of both circuits and the ambient air temperature of a current operating point. Figure 6 shows the user interface of the software application for the HT-evaporator of the ORC

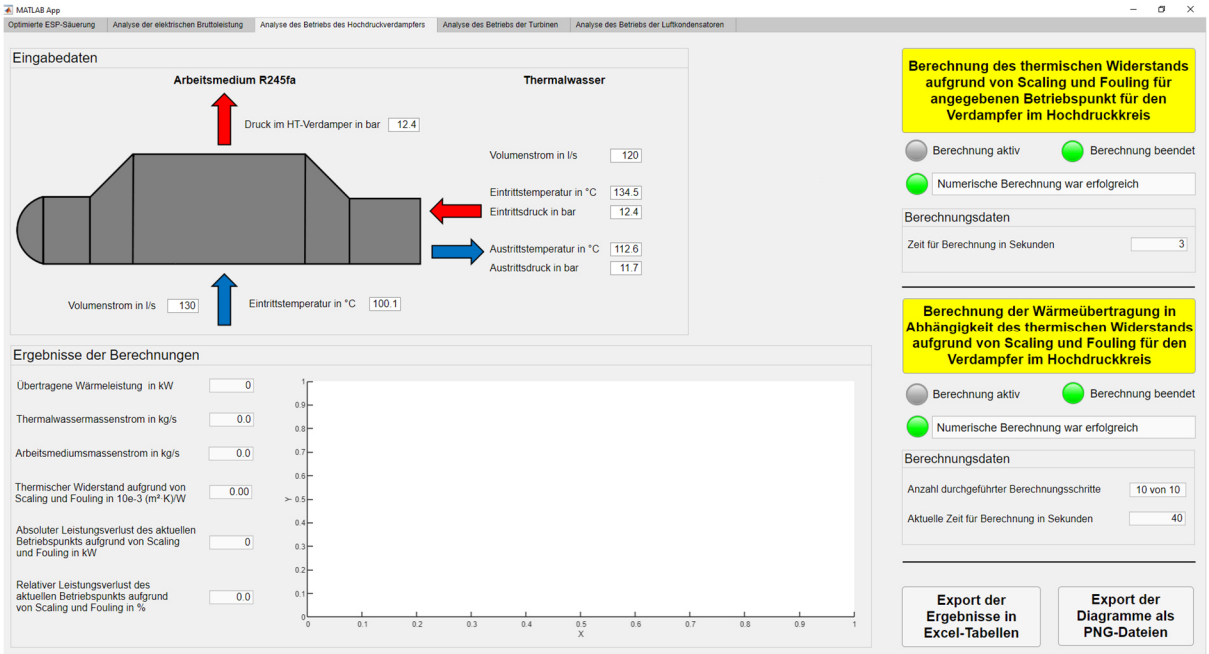

Figure 6: User interface of the software application for the HT-evaporator of the ORC reference geothermal power plant

reference geothermal power plant. The software application calculates the respective thermal resistance due to scaling and fouling of the HT-evaporator, the isentropic turbine efficiencies as well as the enthalpy differences of both turbines, the condensing temperatures as well as the thermal power for desuperheating and condensing of both circuits using the models of the operating years. Furthermore,

the differences between the current values of the key performance indicators and the values of the respective operating year are calculated, which can be used to evaluate the current operating point. All results are plotted graphically and diagrams of the model maps of the isentropic turbine efficiencies and the condensing temperatures for all operating years are part of the software, in which the current operating point is plotted.

7 CONCLUSIONS

In this paper, a methodology is developed and applied to enable easy but sufficiently accurate operation monitoring of the main components of an ORC for geothermal power plant operators. It is shown that the average thermal resistance due to scaling and fouling can be numerically computed as a crucial key performance indicator of the operating state of a large shell-and-tube evaporator using a steady-state equation-based simulation model consisting of only 13 equations in total. The analysis of more than three years of operation of the shell-and-tube evaporator in the high-temperature circuit of the ORC reference geothermal plant shows a minimal thermal resistance due to scaling and fouling for the whole period, which indicates that scaling and fouling did not have a strong influence on heat transfer. Furthermore, applying a two-dimensional polynomial function as an empirical simulation model with the enthalpy difference of the working fluid at the inlet and outlet of a turbine in degree 3 and the mass flow of the working fluid in degree 1 as variables, the isentropic turbine efficiency can be computed with the sum of the difference in magnitude of all residuals to be minimized as objective function with a low RMSE for monitoring the operation of a turbine. Applying the same approach, the condensing temperature can be calculated as a function of the thermal power for desuperheating and condensation of the working fluid and the ambient air temperature with linear dependencies to monitor the operation of air-cooled condensers of ORC power plants. For this empirical simulation model, the best results are obtained using the RMSE as the objective function. Results of applying this methodology by retro perspective analysis of the operational data of a reference geothermal power plant with a two-stage ORC show no negative changes in the operation of the turbines and air-cooled condensers in both circuits of the ORC reference geothermal power plant. A software application enables ORC power plant operators to calculate the key performance indicators and to evaluate and assess the operating states of the main components of their Organic Rankine Cycle power plants with the developed simulation models.

NOMENCLATURE

Letter symbols

A	area	(m²)
C	heat capacity	(J/(kg·K))
d	diameter	(m)
h	enthalpy	(kJ/kg)
$\dot{M}$	mass flow	(kg/s)
p	pressure	(N/m²)
$\dot{Q}$	heat power	(W)
T	temperature	(K)
U	overall heat transfer coefficient	(W/(m²·K))

Greek symbols

α	heat transfer coefficient	(W/(m²·K))
Δ	delta	(-)
ε	surface roughness	(µm)
η	efficiency	(-)
λ	heat conductivity	(W/(m·K))

Subscripts

c	critical
Ev	evaporator
evap	evaporation
HT	high temperature
i	data point
in	inlet
is	isentropic
j	last data point
LT	low temperature
m	mean
mo	model
op	operation
out	outlet
preh	preheating
SaF	scaling and fouling
sat	saturated
T	turbine

Tb	thermal brine
Tp	tube pass
Tu	tube
Wf	Working fluid
x	number of tube pass

REFERENCES

German Geothermal Association, 2021, List of deep geothermal projects in Germany 2020, URL: https://www.geothermie.de/fileadmin/user_upload/Projektliste_Tiefe_Geothermie_2020_KS.pdf, accessed 04.05.2021.

Cooper, M.G., 1984, Heat Flow Rates in Saturated Nucleate Pool Boiling - A Wide-Ranging Examination Using Reduced Properties, Advances in Heat Transfer, vol. 16, no. 1: p. 157-239.

European Commission, 2020, Committing to climate-neutrality by 2050: Commission proposes European Climate Law and consults on the European Climate Pact, Press release on 4th of March 2020, Brussels, URL: https://ec.europa.eu/commission/presscorner/detail/en/ip_20_335, accessed 04.05.2021.

Gnielinski, V., 1975, Neue Gleichungen für den Wärme- und Stoffübergang in turbulent durchströmten Rohren und Kanälen. Forsch. Ing.-Wes., vol. 41, no. 1: p. 8-16.

Irl, M., Schifflechner, C., Wieland., C., Spliethoff, H., 2020, Impact of Scaling on Electrical Submersible Pumps concerning Heat and Power Production of Geothermal Plants and Optimization of Acidification Intervals, *World Geothermal Congress*.

Irl, M., Wieland, C. Spliethoff, H., 2021, Development of an Advanced Monitoring Application for the Power and Efficiency of Air-cooled Geothermal Power Plants, *ECOS 2021*.

Karwa, R., 2020, *Heat and Mass Transfer - Second edition*, Springer Nature Singapore Pte Ltd., Singapore, p. 988-998.

Köhl, B., Elsner, M., Baumann, T., 2020, Hydrochemical and operational parameters driving carbonate scale kinetics at geothermal facilities in the Bavarian Molasse Basin, *Geothermal Energy*, vol. 8, no. 26: p. 2-27.

Mraz, E., 2019, Reservoir Characterization to Improve Exploration Concepts of the Upper Jurassic in the Southern Bavarian Molasse Basin, *Dissertation*, Technical University of Munich.

Smith, D.M., 1934, Mean temperature difference in cross flow. *Engineering*, vol. 138, no. 1: p. 479-481 and p. 606-607.

World Meteorological Organization, 2021, *State of the Global Climate 2020*, Publications Board World Meteorological Organization, WMO-No. 1264, Geneva, p. 5-32.

ACKNOWLEDGEMENT

Funding from the Bavarian State Ministry of Education, Science and the Arts in the framework of the project Geothermal-Alliance Bavaria is gratefully acknowledged. Furthermore, we would also like to show our gratitude to the Munich City Utilities (Stadtwerke München - SWM), which have provided significant support for our research by providing long-term operational data of their geothermal plants as well as useful knowledge and information.